Geosciences and Engineering, Vol. 5, No. 8 (2016), pp. 7–21.

INTERPRETATION OF SELF-POTENTIAL ANOMALIES BY DEVELOPING AN APPROACH BASED ON LINEAR OPTIMIZATION

JAMAL ASFAHANI*–MUHAMMAD TLAS*

**Atomic Energy Commission, P. O. Box 6091, Damascus, Syria*
E-mail: cscientific@aec.org.sy (J Asfahani)

Abstract: A new practical approach is proposed for interpreting self-potential anomalies caused by simple geometric-shaped models such as a sphere, vertical cylinder or horizontal cylinder. The proposed approach is mainly based on both deconvolution and linear optimization techniques to best estimate the model parameters, e.g. the depth to the center of a buried structure, the polarization angle and the amplitude coefficient from self-potential anomaly profile. This method was tested on synthetic data sets corrupted by different Gaussian random noise levels to demonstrate the capability and the reliability of the method. The theoretical modeling results acquired show that the estimated parameter values derived by this proposed method are close to the assumed true values of parameters. The validity of this method is also demonstrated using real field self-potential anomalies taken from the United States and Turkey. A comparable and acceptable agreement is shown between the results derived by this approach and those obtained from the real field data information.

Keywords: *Self-potential anomaly. Sphere-like structure. Cylinder-like structure. Deconvolution technique. Linear optimization*

1. INTRODUCTION

The self-potential (SP) method is among the older methods applied to wide applications in sulfide and graphite exploration and in geophysical groundwater investigations. The quantitative interpretation of SP anomalies is usually carried out by approximating the causative source by simple geometrically shaped models (viz, sheet, cylinder, sphere etc). According to the simplified concept, different interpretation techniques are available in the literature for the quantitative interpretation of SP anomalies. The methods proposed by Yungul [1], Paul [2] and Bhattacharya and Roy [3] use certain characteristic points of the anomaly and hence they turned out to be less reliable in most cases. The curve-matching method proposed by Meiser [4] is cumbersome, especially when there are many parameters to be determined. The methods of least-squares involve a series of trials for minimizing the differences between the observed and the computed self-potential values [5], [6], [7]. The interpretation made by methods based on Fourier and Hilbert transforms [8]–[11] are not straightforward and subject to some inevitable errors in the estimation of the parameters, due to the inaccurate estimation of the horizontal location of

origin. Furthermore, these methods are reliable only for very long profiles. Derivative analysis methods involve higher derivative anomaly [12], [13].

In this paper, a practical interpretation method is introduced to interpret self-potential field anomalies and best estimate of model parameters values, e.g. the depth to the center of the body, the polarization angle, and the amplitude coefficient related to a buried sphere, vertical cylinder or horizontal cylinder-like structure. The method is based on the use of the deconvolution technique to avoid the local minima, where the nonlinear optimization problem, which describes the suitable simple geometric-shaped model of structure, is transformed into a linear optimization problem. This linear optimization problem is thereafter solved by the very well-known algorithm in linear optimization called the simplex algorithm of Dantzig [14], where the global minimum is definitely reached.

The reliability and capability of the proposed interpretation method is demonstrated through analyzing synthetic data sets corrupted by different white Gaussian random noise levels of 10 and 15%. The synthetic model results acquired show that the estimated parameter values derived by this proposed method are very close to the assumed true values of parameters.

The validity of this interpretation method is demonstrated thereafter through interpreting real field self-potential anomalies taken from the United States and Turkey. A comparable and acceptable agreement is obtained between the results derived by this method and those yielded by other interpretation methods. The depth obtained by such a proposed method is found to be in a good accordance with that obtained from real field data information.

2. THEORY

Different theoretical self-potential anomalies related to various geological models such as spheres and horizontal or vertical circular cylinders are treated in this research by the proposed interpretative approach.

2.1 Interpretation of self-potential anomaly due to a horizontal cylinder model

The general expression for the self-potential anomaly (V) at any point $P(x)$ along the x-axis of an arbitrary horizontal cylinder-like structure in a Cartesian coordinate system *(Figure 1)* is given according to [3], [15] as

$$V(x_i) = k \frac{x_i \cos\theta + z \sin\theta}{x_i^2 + z^2} \quad (i = 1,...,N), \tag{1}$$

where z is the depth from the surface to the center of the buried body, θ is the polarization angle between the horizontal and the axis of polarization, k is the amplitude coefficient, and $x_i\,(i = 1,....,N)$ is the horizontal position coordinate.

The set of *Equation (1)* consists of N nonlinear equations in function of the parameters k , θ , and z . To avoid this nonlinearity, the following proposed deconvolution technique will be used. First and for simplification, V_i is used instead of $V(x_i)$ $(i = 1,...,N)$ in the rest of this paper.

Multiplying the two sides of Eq. (1) by the term $\left(x_i^2 + z^2\right)$ and arranging them, we obtain

$$V_i x_i^2 + V_i q_1 - x_i q_2 - q_3 = 0 \quad (i = 1,...,N), \tag{2}$$

where

$$q_1 = z^2 \tag{3}$$

$$q_2 = k\cos\theta \tag{4}$$

$$q_3 = kz\sin\theta \tag{5}$$

The optimal solution (q_1, q_2, q_3) of the set of linear equations (2) can be found by solving the following nonlinear optimization problem onto the real space R^3

$$\min_{q \in R^3} f(q) = \sum_{i=1}^{N} \left(V_i x_i^2 + V_i q_1 - x_i q_2 - q_3\right)^2 \tag{6}$$

subject to $q_1 \geq 0$ and q_2, q_3 are free. With q_2, q_3 being free, the variables q_1, q_2, q_3 will be changed as

$$\left.\begin{aligned} q_1 &= p_1 \\ q_2 &= p_2 - p_4 \\ q_3 &= p_3 - p_4 \end{aligned}\right\}, \tag{7}$$

where $p_1, p_2, p_3, p_4 \geq 0$. Introducing these new variables into (6), the following nonlinear optimization problem with nonnegative variables is obtained

$$\min_{p \in R^4} \varphi(p) = \sum_{i=1}^{N} \left(V_i x_i^2 + V_i p_1 - x_i p_2 + x_i p_4 - p_3 + p_4\right)^2 \tag{8}$$

subject to $p_1, p_2, p_3, p_4 \geq 0$. The quadratic objective function $\varphi(p)$ of this nonlinear optimization problem (8) is convex onto the nonnegative orthant of the real space R^4. This mathematically means that any solution $\left(p_1, p_2, p_3, p_4\right) \in R^4$ satisfying the following optimality conditions of Karush-Kuhn-Tuker (*KKT*) [14]

$$\left.\begin{aligned} & p_i \geq 0 \quad \forall i = 1,...,4 \\ & p_i \frac{\partial \varphi(p)}{\partial p_i} = 0 \quad \forall i = 1,...,4 \\ & \frac{\partial \varphi(p)}{\partial p_i} \geq 0 \quad \forall i = 1,...,4 \end{aligned}\right\} \tag{9}$$

will be a global minima of the convex nonlinear optimization problem (8). The *KKT* optimality conditions (9) for the nonlinear optimization problem (8) are satisfied through solving the following linear optimization problem

$$\left.\begin{aligned} & \min \sum_{i=1}^{4} u_i \\ & \textit{subject to } \frac{\partial \varphi(p)}{\partial p_i} - u_i = 0 \quad \forall i = 1,...,4 \\ & p_i, u_i \geq 0 \quad \forall i = 1,...,4 \end{aligned}\right\} \tag{10}$$

or

$$\left.\begin{aligned} & \min \quad u_1 + u_2 + u_3 + u_4 \quad \textit{subject to} \\ & \left(\sum_{i=1}^{N} V_i^{\,2}\right) p_1 - \left(\sum_{i=1}^{N} V_i x_i\right) p_2 - \left(\sum_{i=1}^{N} V_i\right) p_3 + \left(\sum_{i=1}^{N} V_i (1+x_i)\right) p_4 - u_1 = -\left(\sum_{i=1}^{N} V_i^{\,2} x_i^{\,2}\right) \\ & \left(\sum_{i=1}^{N} V_i x_i\right) p_1 - \left(\sum_{i=1}^{N} x_i^{\,2}\right) p_2 - \left(\sum_{i=1}^{N} x_i\right) p_3 + \left(\sum_{i=1}^{N} x_i (1+x_i)\right) p_4 - u_2 = -\left(\sum_{i=1}^{N} V_i x_i^{\,3}\right) \\ & \left(\sum_{i=1}^{N} V_i\right) p_1 - \left(\sum_{i=1}^{N} x_i\right) p_2 - N p_3 + \left(\sum_{i=1}^{N} (1+x_i)\right) p_4 - u_3 = -\left(\sum_{i=1}^{N} V_i x_i^{\,2}\right) \\ & \left(\sum_{i=1}^{N} V_i (1+x_i)\right) p_1 - \left(\sum_{i=1}^{N} x_i (1+x_i)\right) p_2 - \left(\sum_{i=1}^{N} (1+x_i)\right) p_3 + \left(\sum_{i=1}^{N} (1+x_i)^2\right) p_4 - u_4 = \\ & -\left(\sum_{i=1}^{N} V_i x_i^{\,2} (1+x_i)\right) \\ & \qquad p_1, p_2, p_3, p_4, u_1, u_2, u_3, u_4 \geq 0 \end{aligned}\right\}. \tag{11}$$

In *Equation (11)* (p_1, p_2, p_3, p_4) are structural variables, while (u_1, u_2, u_3, u_4) are artificial variables (surplus variables). The artificial variables (u_1, u_2, u_3, u_4) are added only to measure the deviations between the two sides of equations (11) (requirements of the simplex algorithm) and also to define the objective function of the linear optimization problem (11). These variables (u_1, u_2, u_3, u_4) will be dropped when the optimal values of structural variables (p_1, p_2, p_3, p_4) are reached.

The linear optimization problem (11) is thereafter solved by the Simplex algorithm which starts automatically with an initial guess of parameters; zeros for (p_1, p_2, p_3, p_4) and right-hand-side values of *Equation (11)* for (u_1,u_2,u_3,u_4). The Simplex algorithm will find the optimal values of $(p_1, p_2, p_3, p_4,u_1,u_2,u_3,u_4) \in R^8$ which satisfy the *KKT* optimality conditions (9) for the convex nonlinear optimization problem (8) in a bounded number of iterations and consequently the optimal values of $(q_1,q_2,q_3) \in R^3$ by using *Equation 7*.

For more details about the simplex algorithm of Dantzig for linear optimization problems, readers are referred to [14], [16], [17].

Knowing the optimal values of q_1, q_2 and q_3, it will be easy to find the best estimate of the depth from the surface to the center of the buried horizontal cylinder body (z) by using *Equation (3)* as

$$z = \sqrt{q_1}\,. \tag{12}$$

The best estimate of the polarization angle (θ) and the amplitude coefficient (k) can be easily obtained by using simultaneously *Equations (4)* and *(5)* as

$$\theta = \arctan\left(\frac{1}{z}\frac{q_3}{q_2}\right), \tag{13}$$

$$k = \frac{1}{2}\left(\frac{q_2}{\cos\theta} + \frac{q_3}{z\,\sin\theta}\right). \tag{14}$$

2.2. Interpretation of self-potential anomaly due to a vertical cylinder model

The general expression for the self-potential anomaly (V) at any point $P(x)$ along the x-axis of an arbitrary vertical cylinder-like structure in a Cartesian coordinate system *(Figure 1)* is given according to [3] and [15] as

$$V(x_i) = k\,\frac{x_i\cos\theta + z\,\sin\theta}{\left(x_i^{\,2} + z^{\,2}\right)^{\frac{1}{2}}} \quad (i = 1,...,N)\cdot \tag{15}$$

The notations in this expression have the same meaning as those presented in *Equation 1*. Following the same manner as performed for the horizontal cylinder model, the parameters related to the self-potential anomaly produced by a vertical cylinder can be estimated by the following equations

$$z = \sqrt{q_1}\,, \tag{16}$$

$$\theta = \arctan\frac{1}{2z}\left(\sqrt{\frac{q_3}{q_2}} + \frac{1}{2}\frac{q_4 - q_5}{q_2}\right), \tag{17}$$

$$k = \mp\sqrt{\frac{1}{3}\left(\frac{q_2}{\cos^2\theta}+\frac{q_3}{z^2\sin^2\theta}+\frac{q_4-q_5}{z\sin 2\theta}\right)}, \tag{18}$$

where q_1, q_2, q_3, q_4 and q_5 are obtained by solving the following linear optimization problem using the simplex algorithm

$$\left.\begin{aligned}
&\min \quad u_1+u_2+u_3+u_4 \quad \textit{subject to}\\
&\left(\sum_{i=1}^{N}V_i^4\right)q_1-\left(\sum_{i=1}^{N}V_i^2x_i^2\right)q_2-\left(\sum_{i=1}^{N}V_i^2\right)q_3-\left(\sum_{i=1}^{N}V_i^2x_i\right)q_4+\left(\sum_{i=1}^{N}V_i^2x_i\right)q_5-u_1=-\left(\sum_{i=1}^{N}V_i^4x_i^2\right)\\
&\left(\sum_{i=1}^{N}V_i^2x_i^2\right)q_1-\left(\sum_{i=1}^{N}x_i^4\right)q_2-\left(\sum_{i=1}^{N}x_i^2\right)q_3-\left(\sum_{i=1}^{N}x_i^3\right)q_4+\left(\sum_{i=1}^{N}x_i^3\right)q_5-u_2=-\left(\sum_{i=1}^{N}V_i^2x_i^4\right)\\
&\left(\sum_{i=1}^{N}V_i^2\right)q_1-\left(\sum_{i=1}^{N}x_i^2\right)q_2-Nq_3-\left(\sum_{i=1}^{N}x_i\right)q_4+\left(\sum_{i=1}^{N}x_i\right)q_5-u_3=-\left(\sum_{i=1}^{N}V_i^2x_i^2\right)\\
&\left(\sum_{i=1}^{N}V_i^2x_i\right)q_1-\left(\sum_{i=1}^{N}x_i^3\right)q_2-\left(\sum_{i=1}^{N}x_i\right)q_3-\left(\sum_{i=1}^{N}x_i^2\right)q_4+\left(\sum_{i=1}^{N}x_i^2\right)q_5-u_4=-\left(\sum_{i=1}^{N}V_i^2x_i^3\right)\\
&q_1,q_2,q_3,q_4,q_5,u_1,u_2,u_3,u_4\geq 0
\end{aligned}\right\}. \tag{19}$$

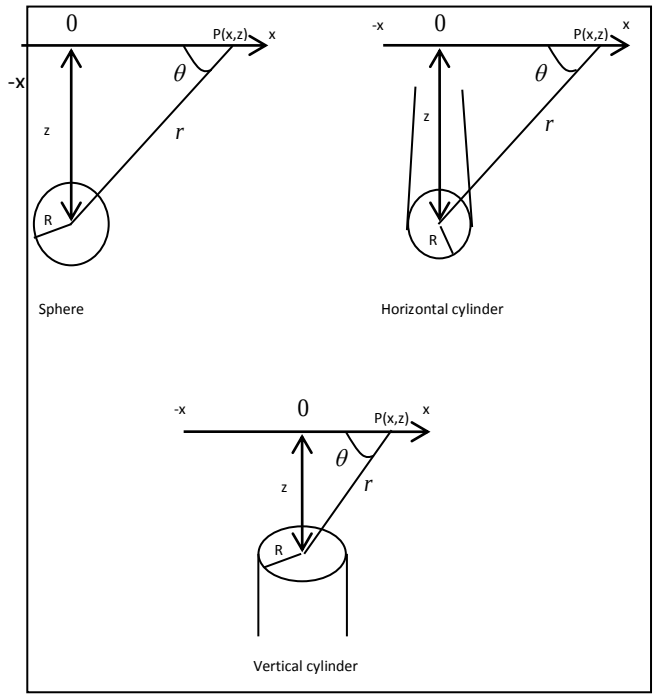

Figure 1. *Diagrams for simple geometrical structures (sphere, horizontal cylinder, and vertical cylinder)*

It is worth noting that the sign of k can be easily assigned by using the statistical criterion of preference called the Root Mean Square Error (RMSE) [18], based on the minimal value between the field data anomaly and the computed one, using the estimated values of z , θ and k . The mathematical formula of this criterion is given as

$$RMSE = \sqrt{\frac{\sum_{i=1}^{N}\left(V_i\left(Observed\right) - V_i\left(Computed\right)\right)^2}{N}},$$

where $V_i\left(Observed\right)$ and $V_i\left(Computed\right)$ $(i = 1,...,N)$ are the observed and the computed self-potential values at the point x_i $(i = 1,...,N)$.

2.3. Interpretation of self-potential anomaly due to a sphere model

The general expression for the self-potential anomaly (V) at any point $P(x)$ along the x-axis of an arbitrary sphere-like structure in a Cartesian coordinate system *(Figure 1)* is given according to [3] and [15] as

$$V(x_i) = k\,\frac{x_i\cos\theta + z\,\sin\theta}{\left(x_i^{\,2} + z^{\,2}\right)^{\frac{3}{2}}} \quad (i = 1,...,N)\cdot \tag{20}$$

The notations in this expression have the same meaning as those presented in *Equation 1*. Following the same manner as performed for the horizontal and vertical cylinder models, the parameters related to the self-potential anomaly produced by a sphere can be estimated by the following equations

$$z = \frac{(q_1)^{\frac{1}{2}} + (q_2)^{\frac{1}{4}} + (q_3)^{\frac{1}{6}}}{3}, \tag{21}$$

$$\theta = \arctan\frac{1}{2z}\left(\sqrt{\frac{q_5}{q_4}} + \frac{1}{2}\frac{q_6 - q_7}{q_4}\right), \tag{22}$$

$$k = \mp\sqrt{\frac{1}{3}\left(\frac{q_4}{\cos^2\theta} + \frac{q_5}{z^{\,2}\sin^2\theta} + \frac{q_6 - q_7}{z\,\sin 2\theta}\right)}, \tag{23}$$

where $q_1, q_2, q_3, q_4, q_5, q_6$ and q_7 are obtained by solving the following linear optimization problem using the simplex algorithm

$$
\begin{aligned}
&\min \quad u_1+u_2+u_3+u_4+u_5+u_6 \quad \textit{subject to}\\
&3\left(\sum_{i=1}^{N}V_i^{\,4}x_i^{\,8}\right)q_1+3\left(\sum_{i=1}^{N}V_i^{\,4}x_i^{\,6}\right)q_2+\left(\sum_{i=1}^{N}V_i^{\,4}x_i^{\,4}\right)q_3-\left(\sum_{i=1}^{N}V_i^{\,2}x_i^{\,6}\right)q_4-\left(\sum_{i=1}^{N}V_i^{\,2}x_i^{\,4}\right)q_5\\
&-\left(\sum_{i=1}^{N}V_i^{\,2}x_i^{\,5}\right)q_6+\left(\sum_{i=1}^{N}V_i^{\,2}x_i^{\,5}\right)q_7-u_1=-\left(\sum_{i=1}^{N}V_i^{\,4}x_i^{\,10}\right)\\
&3\left(\sum_{i=1}^{N}V_i^{\,4}x_i^{\,6}\right)q_1+3\left(\sum_{i=1}^{N}V_i^{\,4}x_i^{\,4}\right)q_2+\left(\sum_{i=1}^{N}V_i^{\,4}x_i^{\,2}\right)q_3-\left(\sum_{i=1}^{N}V_i^{\,2}x_i^{\,4}\right)q_4-\left(\sum_{i=1}^{N}V_i^{\,2}x_i^{\,2}\right)q_5\\
&-\left(\sum_{i=1}^{N}V_i^{\,2}x_i^{\,3}\right)q_6+\left(\sum_{i=1}^{N}V_i^{\,2}x_i^{\,3}\right)q_7-u_2=-\left(\sum_{i=1}^{N}V_i^{\,4}x_i^{\,8}\right)\\
&3\left(\sum_{i=1}^{N}V_i^{\,4}x_i^{\,4}\right)q_1+3\left(\sum_{i=1}^{N}V_i^{\,4}x_i^{\,2}\right)q_2+\left(\sum_{i=1}^{N}V_i^{\,4}\right)q_3-\left(\sum_{i=1}^{N}V_i^{\,2}x_i^{\,2}\right)q_4-\left(\sum_{i=1}^{N}V_i^{\,2}\right)q_5\\
&-\left(\sum_{i=1}^{N}V_i^{\,2}x_i\right)q_6+\left(\sum_{i=1}^{N}V_i^{\,2}x_i\right)q_7-u_3=-\left(\sum_{i=1}^{N}V_i^{\,4}x_i^{\,6}\right)\\
&3\left(\sum_{i=1}^{N}V_i^{\,2}x_i^{\,6}\right)q_1+3\left(\sum_{i=1}^{N}V_i^{\,2}x_i^{\,4}\right)q_2+\left(\sum_{i=1}^{N}V_i^{\,2}x_i^{\,2}\right)q_3-\left(\sum_{i=1}^{N}x_i^{\,4}\right)q_4-\left(\sum_{i=1}^{N}x_i^{\,2}\right)q_5\\
&-\left(\sum_{i=1}^{N}x_i^{\,3}\right)q_6+\left(\sum_{i=1}^{N}x_i^{\,3}\right)q_7-u_4=-\left(\sum_{i=1}^{N}V_i^{\,2}x_i^{\,8}\right)\\
&3\left(\sum_{i=1}^{N}V_i^{\,2}x_i^{\,4}\right)q_1+3\left(\sum_{i=1}^{N}V_i^{\,2}x_i^{\,2}\right)q_2+\left(\sum_{i=1}^{N}V_i^{\,2}\right)q_3-\left(\sum_{i=1}^{N}x_i^{\,2}\right)q_4-Nq_5\\
&-\left(\sum_{i=1}^{N}x_i\right)q_6+\left(\sum_{i=1}^{N}x_i\right)q_7-u_5=-\left(\sum_{i=1}^{N}V_i^{\,2}x_i^{\,6}\right)\\
&3\left(\sum_{i=1}^{N}V_i^{\,2}x_i^{\,5}\right)q_1+3\left(\sum_{i=1}^{N}V_i^{\,2}x_i^{\,3}\right)q_2+\left(\sum_{i=1}^{N}V_i^{\,2}x_i\right)q_3-\left(\sum_{i=1}^{N}x_i^{\,3}\right)q_4-\left(\sum_{i=1}^{N}x_i\right)q_5\\
&-\left(\sum_{i=1}^{N}x_i^{\,2}\right)q_6+\left(\sum_{i=1}^{N}x_i^{\,2}\right)q_7-u_6=-\left(\sum_{i=1}^{N}V_i^{\,2}x_i^{\,7}\right)\\
&q_1,q_2,q_3,q_4,q_5,q_6,q_7,u_1,u_2,u_3,u_4,u_5,u_6\geq 0
\end{aligned}
\qquad . \quad (24)
$$

It is worth noting that the sign of k can be also assigned by using the statistical criterion of preference (RMSE), based on the minimal value between the field data anomaly and the computed one, using the estimated values of z , θ , and k .

2.4. Interpretation of a synthetic self-potential anomaly due to a horizontal cylinder model with different levels of Gaussian random noise

A synthetic self-potential anomaly $V(x_i)\,(i=1,...,N)$ due to a horizontal cylinder-like structure is generated from *Equation (1)* using the following values of model parameters: depth to the center of the structure $z=15$ units length, polarization angle $\theta^o=60$, and the amplitude coefficient $k=100\,mV.m$. This generated synthetic anomaly is perturbed by different Gaussian random noise maximum levels of 10 and 15%, using continuous uniform distribution, where two additional self-potential anomalies are regenerated. Both regenerated self-potential anomalies are consequently interpreted by the new proposed method; estimated model parameters values are shown in *Table 1* and *Figure 2*.

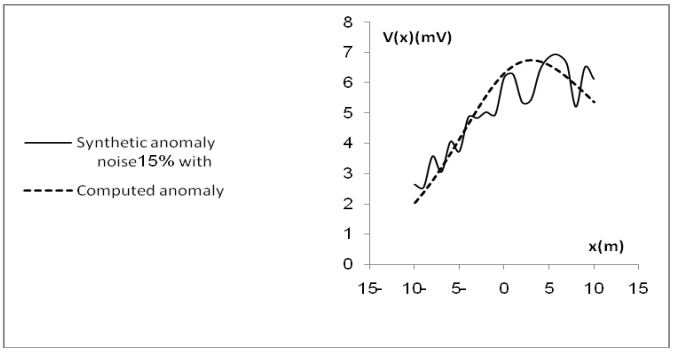

Figure 2. *Diagram for the computed anomaly and synthetic data set adding a maximum random noise of 15%*

Table 1

Interpretation of a synthetic self-potential anomaly due to a horizontal cylinder model with different maximum levels of Gaussian random noise

Model parameters	**True values of model parameters**	**Estimated values of model parameters with maximum 10% random noise**	**Estimated values of model parameters with maximum 15% random noise**
z (unit length)	15	14.05	11.85
θ^0	60	59.49	61.93
k $(mV.m)$	100	96.97	85.12

The results presented in *Table 1* show that the estimated parameter values derived by this interpretation method, are very close to the true values of parameters, which clearly indicates the efficiency and the capability of the proposed interpretation method.

3. APPLICATION TO FIELD DATA

Two field self-potential anomalies over various geological structures are interpreted by the proposed method as follows.

3.1. Interpretation of the Malachite anomaly

Figure 3 shows a self-potential field anomaly measured over the Malachite mine, Jefferson County, Colorado, USA [19], [20]. This self-potential anomaly has been reinterpreted by the proposed method by adapting a priori the three discussed models: a horizontal cylinder, a vertical cylinder, and a sphere as sources of the SP anomaly. The estimated values of the three models parameters and the values of the statistical criterion of preference (RMSE) are explained in *Table 2*.

Table 2

Interpretation of the Malachite mine anomaly, Colorado, USA

Model parameters	Horizontal cylinder	Vertical cylinder	Sphere
z (m)	37.24	12.79	Optimization
θ^0	66.48	79.50	Problem (24) is
k	–7802.31($mV.m$)	–231.90(mV)	not
$RMSE$ (mV)	15.57	14.95	feasible

It can be concluded from *Table 2* that the sphere source causing this anomaly cannot be accepted as a SP model, because the simplex algorithm indicates clearly that linear optimization (24) is infeasible. The minimal value of the Root Mean Square Error ($\mathrm{RMSE} = 14.95$) has been obtained for the vertical cylinder model, meaning that the self-potential anomaly could be preferably modeled as a vertical cylinder with the following parameter values

$$z = 12.79\,m, \quad \theta^o = -79.50, \quad k = 231.90\,mV$$

The depth to the center of the vertical cylinder ($z = 12.79\ m$) is found to be in very good agreement with that obtained from drilling ($z = 13.7\ m$). The computed self-potential anomaly has been drawn according to these estimated values of model parameters as shown in *Figure 3*. The comparison between field and computed

anomalies clearly indicates the close agreement between them, which attests to the capability and the validity of the proposed method.

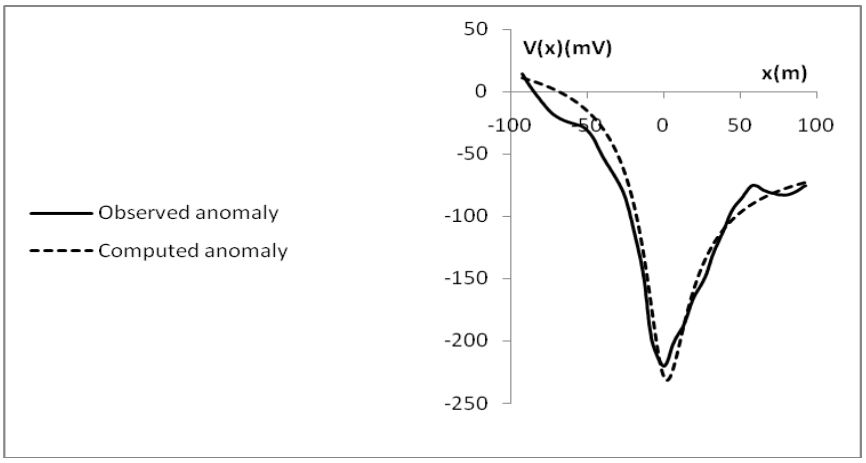

Figure 3. *Self-potential field anomaly over Malachite mine, Colorado, USA. The computed anomaly by the proposed interpretation method is also shown*

3.2. Interpretation of the Sariyer anomaly

Figure 4 shows a self-potential field anomaly measured over a sulfide ore deposit, Sariyer, Turkey [19]–[21]. This self-potential anomaly has been also reinterpreted by the proposed method by adapting a priori the three previous models; a horizontal cylinder, a vertical cylinder and a sphere as sources of the *SP* anomaly. The estimated values of parameters of the three models and the values of the statistical criterion of preference (RMSE) are shown in *Table 3*.

Table 3

Interpretation of the sulfide ore deposit anomaly, Sariyer, Turkey

Model parameters	**Horizontal cylinder**	**Vertical cylinder**	**Sphere**
z (m)	22.58	Optimization	8.88
θ^0	–82.99	Problem (19) is	–5.82
k	4695.60 $(mV.m)$	not	114550 $(mV.m^2)$
$RMSE$ (mV)	14.47	feasible	260.42

It can be concluded from *Table 3* that the source causing this anomaly cannot be modeled as a vertical cylinder, because the simplex algorithm indicates clearly that linear optimization (19) is infeasible. The minimal value of the Root Mean Square Error ($\mathrm{RMSE} = 14.47$) has been obtained for the horizontal cylinder model, mean-

ing that the self-potential anomaly could be preferably modeled as a horizontal cylinder with the following parameter values

$$z = 22.58\,m, \quad \theta^o = -82.99, \quad k = 4695.60\,mV\,.m\,.$$

The depth to the center of the horizontal cylinder ($z = 22.58\,m$) is found to be in very good agreement with that obtained from drilling ($z = 23\,m$). The computed self-potential anomaly has been drawn according to these estimated values of model parameters as shown in *Figure 4*. The comparison between field and computed anomalies clearly indicates the close agreement between them, which attests to the validity of the proposed method.

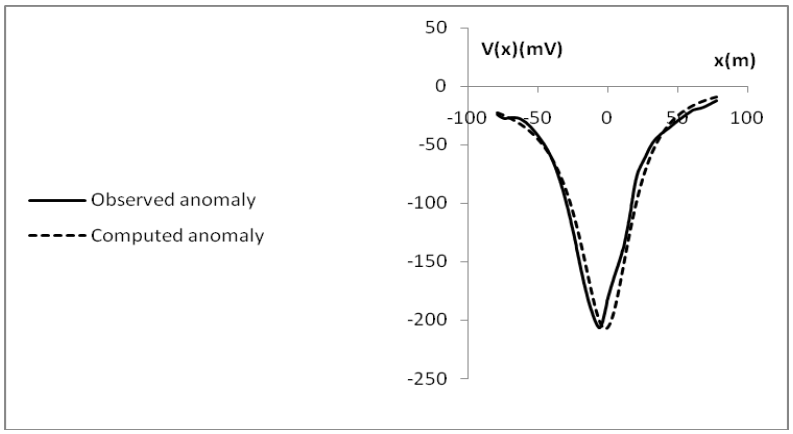

Figure 4. *Self-potential field anomaly over a sulfide ore deposit, Sariyer, Turkey. The computed anomaly by the proposed interpretation method is also shown*

3.3. Discussion

It is useful to mention that there is no loss of generality in assuming the source geometry of the SP anomaly is a priori known. There are in addition no imposed restrictions on the generality of the proposed interpretation method. When the source geometry of the self-potential field anomaly is unknown, three steps must be followed.

First, the self-potential field anomaly is interpreted by adapting the source geometry as a vertical cylinder, where the Root Mean Square Error $\mathrm{RMSE}(1)$ is computed between the observed field anomaly and the computed one.

Second, the self-potential field anomaly is re-interpreted by adapting the source geometry as a horizontal cylinder, where the Root Mean Square Error $\mathrm{RMSE}(2)$ is computed between the observed field anomaly and the computed one.

Third, the self-potential field anomaly is re-interpreted by adapting the source geometry as a sphere, where the Root Mean Square Error $\mathrm{RMSE}(3)$ is computed between the observed field anomaly and the computed one.

The lowest of the three values of RMSE(1), RMSE(2) and RMSE(3) is selected as the solution that exactly indicates the suitable source geometry related to the responsible SP field anomaly.

4. CONCLUSION

In this paper a practical method is proposed for interpreting self-potential anomalies for simple geometric-shaped models such as horizontal cylinder, vertical cylinder, and sphere. The proposed method is based on both the deconvolution technique to avoid local minima and on the simplex algorithm for linear optimization to best estimate the model parameters values, e.g. the depth to the center of the buried structure, the polarization angle and the amplitude coefficient from the self-potential anomaly profile.

The reliability and capability of this interpretation method were first demonstrated through testing and corrupting the synthetic data sets by different white Gaussian random noise levels of 10 and 15%. The synthetic modeling results obtained indicate that the estimated parameter values derived by this new proposed method are very close to the assumed true values of parameters.

The validity of this method is also verified through reinterpreting real field self-potential anomalies taken from the United States and Turkey. A comparable and acceptable agreement is noticed between the results derived by the proposed method and those obtained by other interpretation methods. Moreover, the depth obtained by such a method is found to be in a good accordance with that obtained from the real field data information.

This interpretation method can be easily put into a MATLAB code. Furthermore, since the method is based on the familiar algorithm in linear optimization called the simplex algorithm of Dantzig, convergence towards the best estimation of parameter values is assured and rapidly reached.

This new methodology is therefore recommended for routine analysis of self-potential anomalies in an attempt to determine the best-estimate values of parameters related to different structures under investigation.

ACKNOWLEDGMENTS

Authors would like to thank Dr. I. Othman, Director General of the Syrian Atomic Energy Commission, for his continuous encouragement and guidance to achieve this research. Two anonymous reviewers are deeply thanked for their suggestions and remarks, which considerably improve the final version of this paper.

REFERENCES

[1] YUNGUL, S.: Interpretation of spontaneous polarization anomalies caused by spherical ore bodies. *Geophysics*, 1950, 15. 237–246.

[2] PAUL, M. K.: Direct interpretation of self-potential anomalies caused by inclined sheets of infinite extension. *Geophysics*, 1965, 30. 418–423.

[3] BHATTACHARYA, B. B.–ROY, N.: A note on use of a Nomogram for self-potential anomalies. *Geophysical Prospecting*, 1981, 29, 102–107.

[4] MEISER, P.: A method of quantitative interpretation of self-potential measurements. *Geophysical Prospecting*, 1962, 10, 203–218.

[5] SHALIVAHAN–Bimalendu, B, BHATTACHARYA–Mrinal, K. SEN.; Interpretation of self-potential anomalies by nonlinear inversion. *Journal of Geophysics*, 1998, 19(4), 219–224.

[6] ABDELRAHMAN, E. S. M.–EL-ARABY, T. M.–AMMAR, A. A.–HASSANEIN, H. I.: A least-squares approach to shape determination from residual self-potential anomalies. *Pure and Applied Geophysics*, 1997, 150, 121–128.

[7] ABDELRAHMAN, E. S. M.–SHARAFELDIN, S. M.: A least-squares approach to depth determination from self-potential anomalies caused by horizontal cylinders and spheres. *Geophysics*, 1997, 62, 44–48.

[8] ATCHUTA, Rao–RAM BABU–SIVAKUMAR SINHA, G. D. J.: A Fourier transform method for the interpretation of self-potential anomalies due to two to two-dimensional inclined sheets of finite depth extent. *Pure and Applied Geophysics*, 1982, 120, 365–374.

[9] SUNDARARAJAN, N.–ARUN KUMAR, I.–MOHAN, N. L.–SESHAGIRI RAO, S. V.: Use of Hilbert transform to interpret self-potential anomalies due to two dimensional inclined sheets. *Pure and Applied Geophysics*, 1990, 133, 117–126.

[10] SUNDARARAJAN, N.–SRINIVAS. Y.: A modified Hilbert transform and its application to self-potential interpretation. *Journal of Applied Geophysics*, 1996, 36, 137–143.

[11] SUNDARARAJAN, N.–SRINIVASA RAO, P.–SUNITHA, V.: An analytical method to interpret self-potential anomalies caused by 2-D inclined sheets. *Geophysics*, 1998, 63(5), 1551–1555.

[12] ABDELRAHMAN, E. M.–AMMAR, A. A.–HASSANEIN, H. I.–HAFEZ, M. A.: Derivative analysis of *SP* anomalies. *Geophysics*, 1998, 63, 890–897.

[13] ABDELRAHMAN, E. M.–EL-ARABI. H. M.–HASSANEEN. A. R.–HAFEZ. M. A.: New methods for shape and depth determinations from *SP* data. *Geophysics*, 2003, 68, 1202–1210.

[14] PHILLIPS D. T.–RAVINDRA A.–SOLBER J. J.: Operations Research. John Wiley and Sons, Inc., 1976.

[15] TLAS, M.–ASFAHANI, J.: An approach for interpretation of self-potential anomalies due to simple geometrical structures using Fair function minimization. *Pure and Applied Geophysics*, 2012, 169.

[16] HILLIER, F.–LIEBERMAN, G. J.: Introduction to Operations Research. Holden-Day, Inc., 1986.

[17] BRADLEY, S. P.–HAX, A. C.–MAGNANTI, T. L.: Applied Mathematical Programming. Addison-Wesley, 1977.

[18] COLLINS, G. W.: Fundamental Numerical Methods and Data Analysis. Case Western Reserve University, 2003.

[19] DOBRIN, M. B.: Introduction to geophysical prospecting. Mc Graw-Hill Book Company, Inc., 1960.

[20] ABDELRAHMAN, E. M., SABER, H. S., ESSA, K. S., and FOUDA, M. A.: A least-squares approach to depth determination from numerical horizontal self-potential gradients. *Pure and Applied Geophysics*, 2004, 161, 399–411.

[21] YUNGUL, S.: Spontaneous potential survey of a copper deposit at Sariyer, Turkey. *Geophysics*, 1954, 19, 455–458.